A Hölder-continuous finite-time stable disturbance observer for unmanned vehicles

Pradhyumn Bhale[1], Mrinal Kumar[2], Amit K. Sanyal[1]

***Abstract*— This work provides a finite-time stable disturbance observer design for the discretized dynamics of an unmanned vehicle in three-dimensional translational and rotational motion. The dynamics of this vehicle is discretized using a Lie group variational integrator as a grey box dynamics model that also accounts for unknown additive disturbance force and torque. Therefore, the input-state dynamics is partly known. The unknown dynamics is lumped into a single disturbance force and a single disturbance torque, both of which are estimated using the disturbance observer we design. This disturbance observer is finite-time stable (FTS) and works like a real-time machine learning scheme for the unknown dynamics.**

I. Introduction

In recent years, unmanned aerial vehicles (UAVs) have been increasingly used in several applications ranging from security and monitoring, infrastructure inspection, agriculture and wildland management to package delivery, remote sensing and space and underwater exploration. All these applications have challenges, mainly due to the presence of obstacles and turbulence induced by air flow around structures or regions. In particular, the flight of a UAV over a wildland fire is subjected to unsteady and turbulent airflow, higher temperatures and variable density of air in such regions. These effects affect the flight of the UAVs creating disturbances in the form of perturbations in its flight dynamics, and bring adverse effects in the control performance of these UAVs [1], [2]. Because of these disturbances, a major challenge is to develop a complete model of the dynamics of the UAV being controlled in real time. To add to it, as the complexities of the dynamic systems and their applications increase, the difficulty in modeling uncertain dynamics becomes increasingly important.

This work adds a unique and valuable approach to the numerous approaches proposed in research on control and observer designs for uncertain systems over the last two decades. These approaches are quite varied and use techniques like neural nets, fuzzy logic and soft computing to learn the uncertainties in the dynamics [3]–[7]. More recently, a data-enabled predictive control ("DeePC") scheme [8] was formulated for data-driven control of systems with uncertain dynamics which is similar to the classical model-predictive control (MPC) technique for model-based control system designs of linear systems. Other data-driven approaches that use disturbance or uncertainty observers have also been treated in [9], [10].

It is of critical importance in such applications of UAVs to ensure nonlinearly stable and robust flight, with guaranteed stability margins. Stability of the scheme requires that the identified unknown dynamics changes by a small amount with small changes to inputs and/or outputs. Robustness requires that bounded changes to (or disturbances acting on) the unknown dynamics of system lead to bounded changes in the identified dynamics. In disturbance observer designs for uncertain systems, lack of guaranteed stability is a major shortcoming. For this purpose, a finite-time stable disturbance observer is proposed in this work. This disturbance observer law is both finite-time stable and is obtained in discrete time, making it convenient for onboard computation and implementation.

Disturbance observers [11] [12] (DO) are advantageous in the design of robust control. The idea of a "disturbance-observer" has been around for some time and its origin [13] can be traced back to the early 1970s. They are commonly used to estimate uncertainties in nonlinear systems as they are easy, intuitive and possess a simple structure. Their main role is to estimate the disturbance inputs (uncertainties) to the dynamics. This helps in creating a modular design of controllers where an outer loop controller can be designed for the nominal plant and the disturbance estimate from the DO is used to compensate it [14]. In this regard, a disturbance observer has an advantage over other control methods like $\mathcal{H}_\infty$ control, adaptive control, or sliding mode control. Also, it offers a much larger design freedom for the controller design that works in the outer-loop. The main aim of this paper is to obtain a finite-time stable observer design for stable and robust learning of unsteady and unknown aerodynamic effects on UAV flight dynamics.

DO-based techniques can provide a feasible way to improve robustness and deal with disturbances or uncertainties of nonlinear systems in real time. The finite-time stable disturbance observer (FTSDO) obtained here has a faster convergence rate and better disturbance rejection abilities than conventional nonlinear DO. In other words, the finite-time stable (FTS) disturbance (output) observer can be designed to converge in a finite-time period that is smaller than the settling time of the controller. One other aspect of FTS designs is that they provide guaranteed convergence. Systems with dynamics that have a finite settling-time are more robust to bounded changes to system dynamics than asymptotically stable designs [15], [16].

The DO approach follows from the recent work [17],

[1] Department of Mechanical and Aerospace Engineering, Syracuse University, Syracuse, NY, 13244, USA. pbhale, aksanyal@syr.edu

[2] Department of Mechanical and Aerospace Engineering, The Ohio State University, Columbus, OH, 43210, USA. kumar.672@osu.edu

which developed a finite-time stable disturbance observer in discrete-time for a generalized MIMO system represented by an ultra-local model [18]. Unlike prior work, here we treat the complete 6-DoF dynamics for a UAV on the Lie group of rigid body motions $\mathrm{SE}(3)$, using a disturbance observer. Part of the dynamics model for the UAV is known and the unknown (disturbance) inputs are given by the disturbance observer; together they make up a grey box model for the input-state dynamics. All the unknown dynamics of the model are combined into two terms, the disturbance force and the disturbance torque. The discretization of the equations of motion for the rigid body in $\mathrm{SE}(3)$ are carried out in the framework of discrete geometric mechanics, and the resulting discrete-time equations are in the form of a Lie group variational integrator (LGVI) [19] [20]. The Lie group variational integrator is globally defined on the nonlinear state space $\mathrm{SE}(3) \times \mathbb{R}^6$. As they are known to preserve energy-momentum properties and the geometry of the Lie group without any need of local projections, LGVI schemes are ideal for this application [21].

An important aspect of this formulation is that local coordinates or quaternions are not used to represent the attitude on $\mathrm{SO}(3)$. The observer is constructed to be finite-time stable (FTS) on the space of rigid body motions, $\mathrm{SE}(3)$ which is the semi-direct product of $\mathbb{R}^3$ and $\mathrm{SO}(3)$ [22]. One adverse consequence of unstable estimation and control schemes is that, if they converge or settle, they end up taking longer to converge compared to stable schemes with the same initial conditions and same initial transient behavior [23], [24]. Attitude and pose observers and filtering schemes on $\mathrm{SO}(3)$ and $\mathrm{SE}(3)$ have been reported in, e.g., [25]–[29]. Prior work on observer design and estimation directly on the Lie groups of rigid body motions can be found in [30]–[32].

A brief outline of this paper is given here. In Section II, we give some preliminaries regarding rigid body motion. The discretization of the kinematics and dynamics are given in Section III using the discrete-time Lagrange d'Alembert principle. Section IV covers the main results for designing a finite-time stable disturbance observer to estimate the unknown dynamics. It relates the observed outputs to the given inputs and estimates the unknown disturbance dynamics using the (estimated) internal states and known (control) inputs. Numerical simulation results based on a LGVI scheme for the observer discretization are demonstrated in Section V. We conclude the paper, in Section VI, by summarizing the results and highlighting possible future research directions.

II. Preliminaries

A. Lie Group of Rigid Body Motions $\mathrm{SE}(3)$

The set of possible configurations for a 6 degree of freedom (DOF) rigid body is the Lie group of rigid body motions, denoted by $\mathrm{SE}(3)$. The group $\mathrm{SE}(3)$ is the semi-direct product of $\mathbb{R}^3$ and the special orthogonal group of rigid body orientations $\mathrm{SO}(3)$, i.e., $\mathrm{SE}(3) = \mathbb{R}^3 \times \mathrm{SO}(3)$ [33]. The configuration of a rigid body is given by its position vector from the origin of an inertial coordinate frame $\mathcal{I}$ to the origin of a body-fixed coordinate frame $\mathcal{B}$ denoted $b \in \mathbb{R}^3$, and its attitude described by the rotation matrix from body-fixed frame $\mathcal{B}$ to the inertial frame $\mathcal{I}$ denoted by $\mathbb{R} \in \mathrm{SO}(3)$.

The special orthogonal group of rigid body rotation, $\mathrm{SO}(3)$ [34], is defined by:

$$\mathrm{SO}(3) = \left\{ R \in \mathbb{R}^{3\times 3},\ R^{\mathrm{T}}R = RR^{\mathrm{T}} = I,\ \det(R) = 1 \right\}.$$

$\mathrm{SO}(3) \subset \mathbb{R}^{3\times 3}$ is a matrix Lie group under matrix multiplication. The Lie algebra (tangent space at identity) of $\mathrm{SO}(3)$ is denoted $\mathfrak{so}(3)$ and defined as,

$$\mathfrak{so}(3) = \left\{ S \in \mathbb{R}^{3\times 3} \mid S + S^T \right\},$$
$$S = s^{\times} = \begin{bmatrix} 0 & -s_3 & s_2 \\ s_3 & 0 & -s_1 \\ -s_2 & s_1 & 0 \end{bmatrix}.$$

Here $(.)^{\times} : \mathbb{R}^3 \to \mathfrak{so}(3)$ denote the bijective map from three dimensional Euclidean space to $\mathfrak{so}(3)$. For a vector $s = [s_1\ s_2\ s_3]^{\mathrm{T}} \in \mathbb{R}^3$, the matrix $s^{\times}$ represents the vector cross product operator, that is $s \times r = s^{\times} r$, where $r \in \mathbb{R}^3$. The inverse of $(.)^{\times}$ is denoted $\mathrm{vex}(.) : \mathfrak{so}(3) \to \mathbb{R}^3$, such that $\mathrm{vex}(a^{\times}) = a$, for all $a^{\times} \in \mathfrak{so}(3)$. Together with the position vector of the (center of mass) of the rigid body, its pose (position and orientation) is given by:

$$g = \begin{bmatrix} R & b \\ 0 & 1 \end{bmatrix} \in \mathrm{SE}(3). \tag{1}$$

B. System Kinematics and Dynamics

The instantaneous pose (position and attitude) is compactly represented by $g = (b, R) \in \mathrm{SE}(3)$. Denoting the time derivative by $\dot{()}$, the kinematics of the UAV is given by:

$$\begin{cases} \dot{b} = v = R\nu, \\ \dot{R} = R\Omega^{\times}, \end{cases} \tag{2}$$

where $v \in \mathbb{R}^3$ and $\nu \in \mathrm{R}^3$ denote the translational velocity in frames $\mathcal{I}$ and $\mathcal{B}$ respectively, and $\Omega \in \mathbb{R}^3$ is the angular velocity in frame $\mathcal{B}$. The dynamics of a rotorcraft UAV with a body-fixed plane of rotors is given by:

$$\begin{cases} m\ddot{b} = m\dot{v} = (f^c R - mg)e_3 + \phi_d, \\ J\dot{\Omega} = \tau^c - \Omega^{\times} J\Omega + \tau^d, \end{cases} \tag{3}$$

where $e_3 = [0\ 0\ 1]^{\mathrm{T}}$, $f^c \in \mathbb{R}$ is the scalar thrust force and $\tau^c \in \mathbb{R}^3$ is the control torque created by the rotors, g denotes the acceleration due to gravity and $m \in R^+$ and $J = J^{\mathrm{T}} \in \mathbb{R}^{3\times 3}$ are the mass and inertia matrix of the UAV, respectively. The disturbance force and torque are denoted ϕ^d and τ^d respectively, which are mainly due to unsteady aerodynamics in this application. This dynamics model is expressed in discrete time for real-time identification of these disturbances and their compensation for tracking control in the next section using an LGVI scheme.

III. Problem Formulation for Disturbance Observer on SE(3)

A. Discrete-time Dynamics:

Let f_k denote the discrete approximation to a continuous time-varying quantity f at time $t_k = t(k)$. Let us denote $h \neq 0$ as the fixed step size, i.e., $t_{k+1} - t_k = h$. A discrete Lagrangian $\mathcal{L}$ approximates a segment of the action integral:

$$\mathcal{L} \approx \int_{t_k}^{t_{k+1}} \mathcal{L}(b, \nu, R, \Omega)\, dt,$$

Similarly, we construct $\mathcal{F}$ to approximate a segment of the virtual work integral and then, the discrete dynamics is prescribed by the discrete Lagrange-d'Alembert principle:

$$\delta \sum_{k=0}^{N-1} \mathcal{L}_k + \sum_{k=0}^{N-1} \mathcal{F}_k = 0, \tag{4}$$

Defining the inner product as the trace pairing $\langle ., . \rangle$: $\mathbb{R}^{n\times m} \times \mathbb{R}^{n\times m}$ given by:

$$\langle A, B \rangle := tr(A^T B).$$

The discrete-Lagrangian is chosen as the approximation:

$$\mathcal{L}_k(b, \nu, R, \Omega) = \frac{h}{2}\langle M\nu_k, \nu_k \rangle + \frac{h}{2}\langle J\frac{1}{h}(\exp(h\Omega_k^\times) - I), \exp(h\Omega_k^\times) - I\rangle - \frac{h}{2}\big(\mathcal{U}(b_k, R_k) + \mathcal{U}(b_{k+1}, R_{k+1})\big), \tag{5}$$

where J is the inertia matrix, M is the mass matrix for the body and $\mathcal{U}(b, R) : \mathrm{SE}(3) \to \mathbb{R}$ denotes the potential energy function, which in the case of an UAV in flight is given by uniform gravity:

$$\mathcal{U}(b, R) := \mathcal{U}(b) = mgb^{\mathrm{T}} e_3. \tag{6}$$

The infinitesimal variations $\delta b, \delta\nu, \delta R$ and $\delta exp(\Omega_k^\times)$ are given by:

$$\begin{cases} \delta b_k = R_k \gamma_k, \\ \delta R_k = R_k \Sigma_k^\times, \\ \delta \exp(\Omega_k^\times) = -\Sigma_k^\times \exp(\Omega_k^\times) + \exp(\Omega_k^\times)\Sigma_{k+1}^\times, \\ \delta\nu_k = \frac{1}{h} R_k^T(\delta b_{k+1} - \delta b_k) - \Sigma_k^\times \nu_k, \end{cases} \tag{7}$$

where Σ and γ vanish at the end points but are otherwise arbitrary. Using these, for $\mathcal{F}$, we choose an approximation of the form:

$$\mathcal{F}_k = \frac{h}{2}\langle \tau_k^\times, \Sigma_{k+1}^\times \rangle + h\langle \psi_k, R_{k+1}\delta b_{k+1} \rangle, \tag{8}$$

where τ and ψ denote the nonconservative moments and forces, respectively. Next, we get the discrete kinematic equations as a first order forward Euler discretization of eq. (2), to get:

$$\begin{cases} b_{k+1} = b_k + hR_k\nu_k, \\ R_{k+1} = R_k \exp(h\Omega_k^\times), \end{cases} \tag{9}$$

Using the discrete Lagrange d'Alembert principle in (4), we get the discretized dynamic equations as:

$$\begin{cases} m\nu_{k+1} = hR_{k+1}^T(f_k^c - mg)e_3 + h\phi_k^d, \\ J\Omega_{k+1} = h\tau_k^c + exp(-h\Omega_k^\times)J\Omega_k + h\tau_k^d, \end{cases} \tag{10}$$

where the whole number subscript $k \in \mathbb{W}$ denotes the time variable corresponding to the sampling instant t_k. These equations are obtained in the form of a Lie group variational integrator, and the matrix exponential in (10) is evaluated using the Rodrigues formula for numerical efficiency. Using Rodrigues' formula gives:

$$\exp(h\Omega^\times) = I + \frac{\sin\|h\Omega\|}{\|h\Omega\|}(h\Omega^\times) + \frac{1 - \cos\|h\Omega\|}{\|h\Omega\|^2}(h\Omega^\times)^2. \tag{11}$$

For a more detailed use of the discrete Lagrange d'Alembert principle to get the dynamic equations of a rigid body, the reader is directed to these previous works [19] [21]. It is important to note here that the discrete-time equations in (9) and (10) can be extended for variable-time steps and if the sampling period $t_{k+1} - t_k = \Delta t$ is constant, then the equations will give back (9) and (10). This study for variable time step with a more detailed derivation for the discretized equations will be provided in a future work. Some definitions and lemma are stated next before the main theorems in the next section.

Definition 1: Any real-valued function $f : \Omega \to \mathbb{R}$ is Hölder continuous with exponent $\alpha \in$ (0,1) if it satisfies:

$$|f(x) - f(y)| \leq C\,\|x - y\|^\alpha,$$

for all x and y in the domain of f.

Lemma 1: Consider a discrete-time system with outputs $s_k \in \mathbb{R}^p \to \mathbb{R}$ and let $V : \mathbb{R}^p \to \mathbb{R}$ be a corresponding positive definite (Lyapunov) function and denote $V_k := V(s_k)$. Let α be a constant in the open interval]0,1[and $\eta \in \mathbb{R}^+$. Denote $\gamma_k := \gamma(V_k)$ where $\gamma : \mathbb{R}_0^+ \to \mathbb{R}_0^+$ is a positive definite function of V_k. Let γ_k satisfy the condition:

$$\gamma_k \geq \eta := \epsilon^{1-\alpha} \text{ for all } V_k \geq \epsilon. \tag{12}$$

for some constant $\epsilon \in \mathbb{R}^+$. Then, if V_k satisfies the relation:

$$V_{k+1} - V_k \leq -\gamma_k V_k^\alpha, \tag{13}$$

the discrete system is (Lyapunov) stable at $s = 0$ and s_k converges to $s = 0$ for $k > N$, where $N \in \mathbb{W}$ is finite.

Proof: The proof of this lemma is given in [17] and omitted here for brevity. ■

Lemma 2: A discrete-time Lyapunov function that satisfies inequality (13) is Hölder-continuous in discrete time.

Proof: The proof of this lemma is given in [17] and omitted here for brevity. ■

IV. Finite-Time Stable Observer Design

There are different formulations [35], [36] available to estimate the output and state variables in the equations of motion given by (10). These can be used in conjunction with the disturbance observer presented here. In this work,

we assume that reasonably accurate estimates of the output and state variables are available. Using this assumption, the estimation equation for the disturbance forces and torques can be written as:

$$\begin{cases} \phi_k^d = \frac{1}{h}(m\hat{w}_{k+1} - h\hat{R}_{k+1}^T(f_k^c - mg)e_3), \\ \tau_k^d = \frac{1}{h}(J\hat{\Omega}_{k+1} - h\tau_k^c - exp(-h\Omega_k^\times)J\Omega_k). \end{cases} \quad (14)$$

The unknown disturbance inputs $\chi_k^d = (\Phi_k^d, \tau_k^d) \in \mathbb{R}^6$ are learnt in real time according to the past input-output history using (14). Let us denote the error in estimating χ_k as:

$$e_k^\chi := \hat{\chi}_k^d - \chi_k^d. \quad (15)$$

Also, the first order finite difference of the unknown dynamics, χ_k^d, is given by:

$$\Delta\chi_k := \chi_k^{(1)} = \chi_{k+1} - \chi_k \quad (16)$$

Then, the disturbance estimate $\hat{\chi}_{k+1}^d$ can be obtained in real time from the first order nonlinearly stable observer law stated next.

Theorem 1: The nonlinear observer for χ_k given by

$$\hat{\chi}_{k+1}^d = \mathbf{D}(e_k^\chi)e_k^\chi + \chi_k^d, \quad (17)$$

where $\hat{\chi}_0^d = \chi_0^d$ is given and D : $\mathbb{R}^+ \rightarrow$R is a Hölder-continuous function which is designed to make this observer finite-time stable. This observer design leads to finite time stable convergence of the estimation error vector $e_k^\chi \in \mathbb{R}^6$ to a bounded neighborhood of $0 \in \mathbb{R}^6$, where bounds on the neighborhood are obtained from the bounds on ΔF_k.

The Hölder-continuous function D(e_k^χ) is given by:

$$D(e_k^\chi) = \frac{((e_k^\chi)^T e_k^\chi)^{1-1/r} - \lambda}{((e_k^\chi)^T e_k^\chi)^{1-1/r} + \lambda}, \quad (18)$$

where $\lambda > 0$ and r $\in$ (1,2) are constants.

Proof: Consider the discrete-time Lyapunov function

$$V_k^\chi := (e_k^\chi)^T e_k^\chi. \quad (19)$$

Taking the first order discrete-time difference of this Lyapunov function gives us:

$$V_{k+1}^\chi - V_k^\chi = -\gamma_k^\chi (V_k^\chi)^{\frac{1}{r}}, \quad (20)$$

where,

$$\gamma_k^\chi = (1 - (D(e_k^\chi))^2)(V_k^\chi)^{1-\frac{1}{r}}.$$

This implies that γ_k^χ is a positive definite function of $V_k^\chi = \|e_k^\chi\|^2$. Using (19) and (22), we can express γ_k^χ as a function of V_k^χ:

$$\gamma_k^\chi = 4\lambda \frac{(V_k^\chi)^{2-\frac{2}{r}}}{((V_k^\chi)^{1-\frac{1}{r}} + \lambda)^2}. \quad (21)$$

It can be inferred from (21) that $\gamma_k^\chi := \gamma(V_k^\chi)$ is a class-κ function of V_k^χ. Moreover, it can be verified that:

$$\implies V_N^\chi \leq \lambda^{\frac{1}{1-1/r}},$$

$$\implies \gamma_N^\chi \leq \lambda.$$

The last two results together imply that γ_k^χ satisfies the sufficient condition for finite-time stability of e_k^χ as stated in Lemma 1. Now, consider the expression for e_{k+1}^χ given by

$$e_{k+1}^\chi = D(e_k^\chi)e_k^\chi, \quad (22)$$

Using (15) and (22), the following discrete-time disturbance observer for $\hat{\chi}_k$ is obtained:

$$\hat{\chi}_{k+1} = D(e_k^\chi)e_k^\chi + \chi_{k+1}. \quad (23)$$

The above expression leads to a finite-time stable observer for the unknown dynamics that ensures that the estimation error e_k^χ converges to zero for $k > N$ where $N \in \mathbb{W}$ is finite. However, due to the causality of the values from the dynamics, the value of χ_{k+1} is not available at time t_{k+1}, and it needs replacing by a known quantity. Consequently, χ_{k+1} is replaced by χ_k in (23) to obtain the first-order observer design given by (19).

The observer stated in equation (19) is basically a first-order perturbation of the ideal FTS observer design for χ_k as given by (23). The first-order finite difference term $\Delta\chi_k$ is the source of the perturbation in this case. ■

Theorem 2: Consider the nonlinear observer law for the disturbance χ_k given by (17). Let the bound on the first order difference $\Delta\chi_k$ defined by (16) be given by:

$$\|\Delta\chi_k\| \leq B^\chi, \quad (24)$$

where $B_\chi \in \mathbb{R}^+$. Then, the observer estimation error e_k^χ is guaranteed to converge to the neighborhood given by:

$$N^\chi := \{e_k^\chi \in \mathbb{R}^n : \rho(e_k^\chi)\|e_k^\chi\| \leq \mathrm{B}^\chi\}, \quad (25)$$

for finite $k > N$, $N \in \mathbb{W}$, where

$$\rho(e_k^\chi) := 1 + |D(e_k^\chi)|. \quad (26)$$

Proof: Using the Lyapunov equation defined by (13) and the observer equation (19), we obtain

$$V_{k+1} - V_k = ((D(e_k^\chi))^2 - 1)(e_k^\chi)^T e_k^\chi - 2D(e_k^\chi)\Delta\chi_k^T e_k^\chi + \Delta\chi_k^T \Delta\chi_k,$$

Using the bound on the value of $\|\Delta\chi_k\|$ given by (24), we can get an upper bound on the first difference of the Lyapunov function:

$$\Delta V_k^\chi \leq (D^2 - 1)\|e_k^\chi\|^2 + 2|D|B^\chi\|e_k^\chi\| + (B^\chi)^2, \quad (27)$$

where $D := D(e_k^\chi)$ for ease of notation. For large enough initial (transient) $\|e_k^\chi\|$, the right hand side of the inequality (27) is negative, which gives us the following condition:

$$(1 - D^2)\|e_k^\chi\|^2 - 2|D|B^\chi\|e_k^\chi\| - (B^\chi)^2 > 0, \quad (28)$$

The above equation (28) can be considered as a quadratic inequality expression in $\|e_k^\chi\|$ with coefficients that depend on e_k^χ. This leads to the condition,

$$(|D(e_k^\chi)| + 1)\|e_k^\chi\| > B^\chi, \quad (29)$$

for real positive solutions of $\|e_k^\chi\|$ for which $\Delta V_k^\chi < 0$ is guaranteed. Note that $D(e_k^\chi)$ is a monotonically increasing function taking values in the range of [-1, 1). The discrete

Lyapunov function V_k^{χ} will decrease monotonically for $\|e_k^{\chi}\|$ large enough to satisfy inequality (29), which it will until a finite value of k, say $k = N$. Therefore, the observer error is guaranteed to converge to the neighborhood N^{χ} of the zero vector $\in \mathbb{R}^6$ given by equation (25) and will stay in this positively invariant neighborhood for $k > N$. ■

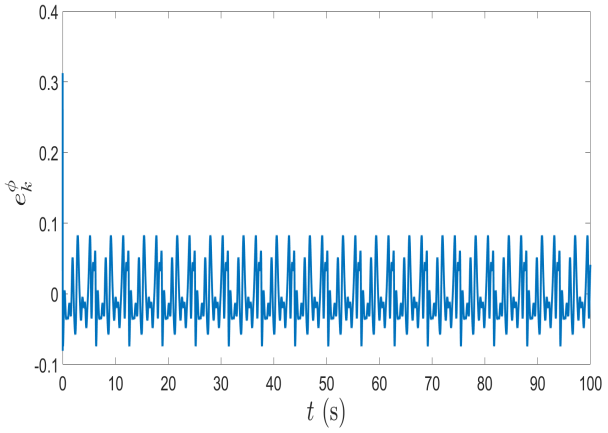

(a) Model estimation error for the magnitude of disturbance force

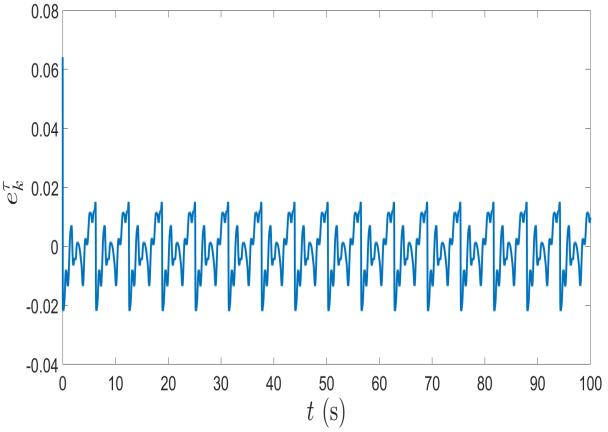

(b) Model estimation errors for disturbance without noise

Fig. 1: Model estimation error for disturbance without noise

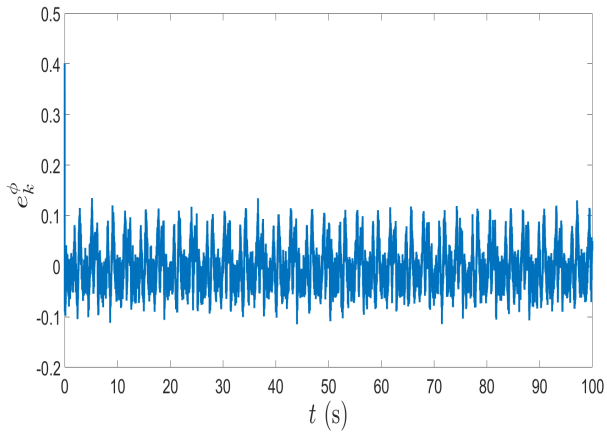

(a) Model estimation error for the magnitude of disturbance force

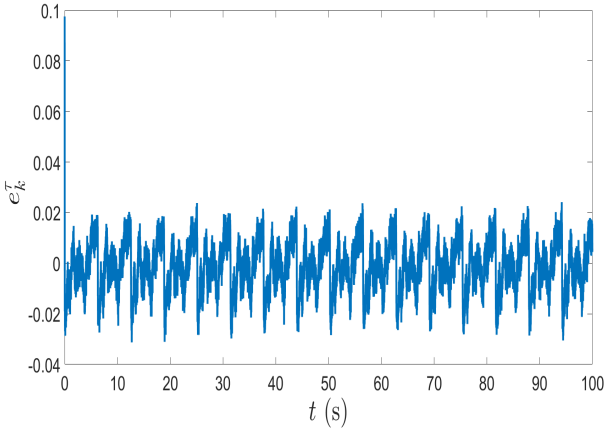

(b) Model estimation error for the magnitude of disturbance torque

Fig. 2: Model estimation errors for disturbance with noise

V. Numerical Simulation

In this section, a comprehensive numerical simulation study for the FTS disturbance observer presented in Theorem 1 is carried out. The disturbance observer is shown to converge in finite-time and is found to be robust to measurement noise. Also, it is shown to be bounded in the neighborhood of the zero vector $\in \mathbb{R}^6$ as given by Theorem 2.

A. Finite-time Convergence

Short-term, turbulent wind effects are difficult to model exactly even with the use of detailed CFD analysis and certain simplifying assumptions for the wind fields are often used. The uncertainties that exist in a realistic wind field contain a variety of different atmospheric sources like turbulence, vortex, gust and shear. Despite this, a combination of sinusoidal wave-forms are generally sufficient to capture the dominant characteristics that exist in a realistic wind field.

To this avail, the wind disturbance is modeled as a combination of sinusoidal frequencies. To make the wind model more realistic and close to the real-world environment, lower frequency signals of relatively higher amplitude are combined with higher frequency signals of relatively lower amplitude, with the frequencies being not more than 10 Hz. The total magnitude of the force and torque disturbance is of the order of ∼5-7 N and ∼1-2 N-m, respectively.

These disturbances are propagated in the system dynamics given by (14). In the simulation, the measurements are generated by numerically propagating the true discrete-time dynamics. For the results in this subsection, no (measurement) noise is added to the outputs and only the finite-time convergence of the disturbance estimates is examined. Output measurements are assumed at a constant rate of 50 Hz, i.e. sampling period Δt = 0.02 s. The unknown disturbance dynamics is obtained from the estimated outputs.

The first order finite-time stable observer stated in Theorem 1 is used for getting the disturbance estimate. The Hölder-continuous function $D(e_k^{\chi})$ defined in (17) is taken

as:

$$D(e_k^\chi) = \frac{((e_k^\chi)^T e_k^\chi)^{1-1/r} - \lambda}{((e_k^\chi)^T e_k^\chi)^{1-1/r} + \lambda}, \tag{30}$$

The observer gains used in this function are:

$$\lambda = 1.0, \text{ and } r = \frac{9}{7}$$

Simulation results for the estimation error in estimating the unknown (disturbance) dynamics are depicted in Figure 1. The disturbance term $\chi_k^d \in \mathbb{R}^6$ comprises of two parts, the disturbance force, $\Phi_k^d \in \mathbb{R}^3$ and the disturbance torque, $\tau_k^d \in \mathbb{R}^3$. Figure 1a and 1b show the estimation error in the magnitude of disturbance force $\|\mathbf{\Phi_k^d}\|$ and disturbance torque $\|\tau_\mathbf{k}^\mathbf{d}\|$, respectively. It can be clearly inferred from the plots that the disturbance estimation error settles down in the neighborhood of the zero vector in finite-time after the initial disturbance and their estimates start away from each other. This validates the finite-time convergence of the first-order nonlinear observer given by (17). This ideal scenario where the outputs don't have any measurement noise associated with them is almost never true and hence, a robustness analysis of the observer is required.

B. Robustness to measurement noise

Generally, the output states have measurement noise associated with them which results in the calculated disturbance measurements using the input-output dynamics (as shown in (14)) being different from the actual disturbance measurements that are acting on the system dynamics. A robust disturbance observer will make the disturbance estimates converge to a bounded neighborhood in the presence of bounded measurement noise.

Here, simulations are carried out in a similar setting as the previous subsection. In this case, the measurements are generated by numerically propagating the true discrete-time dynamics and adding noise to the true outputs. The added noise signals are taken to be ~ 2 % of the true output values which gives a realistic signal-to-noise ratio (SNR) around 30 dB. This is a decent estimate for current day off-the-shelf sensors that are used in the UAV industry and even better performing sensors are available now.

Simulation results for the estimation error with added noise are depicted in Figure 2. Figure 2a and 2b show the estimation error in the magnitude of disturbance force $\|\mathbf{\Phi_k^d}\|$ and disturbance torque $\|\tau_\mathbf{k}^\mathbf{d}\|$, respectively. The numerical results show good finite-time convergence of the disturbance estimation error to a bounded neighborhood of the zero vector, further validating the robustness of the observer design.

C. Convergence bounds for the DO

Theorem 2 gives a bound for the observer estimation error which in turn is dependent on the bound on the first order finite difference of the unknown dynamics, χ_k^d. For the disturbance force Φ_k^d, the total magnitude is of the order of $\sim$ 5-7 N and simulated measurements are taken at a constant rate of 50 Hz, as stated earlier. This gives a bound B^Φ for the first order difference of the disturbance force. Calculating the value of B^Φ and using (24) gives:

$$\|\Delta\Phi_k^d\| \leq 0.14, \tag{31}$$

From (25), we get:

$$\rho(e_k^\Phi)\|e_k^\Phi\| \leq 0.14, \tag{32}$$

Taking the maximum value of e_k^Φ and substituting it in the expression for D(e_k^Φ) given by (30), we get the value of $\rho(e_k^\Phi)$ from (26) as:

$$\rho(e_k^\Phi) \approx 1.5, \tag{33}$$

From (32) and (33), we get:

$$\|e_k^\Phi\| \leq .095, \tag{34}$$

The bounds given for the estimation error for the disturbance force by (34) can be verified from figure 1a and found to be satisfying the limit.

For the disturbance torque, the total magnitude is of the order $\sim$ 1-2 N-m and similarly, the bound for the first order difference of the disturbance torque can be given by:

$$\|\Delta\tau_k^d\| \leq 0.035, \tag{35}$$

Similarly, from (25) we get:

$$\rho(e_k^\tau)\|e_k^\tau\| \leq 0.035, \tag{36}$$

Following the same procedure as for the disturbance force earlier, we get:

$$\rho(e_k^\tau) \approx 1.7, \tag{37}$$

From (36) and (37), we get the bound for the estimation error for the magnitude of disturbance torque given as:

$$\|e_k^\tau\| \leq 0.021 \tag{38}$$

Again, these bounds can be verified from the plot for the estimation error of disturbance torque given in 1b.

VI. Conclusion and Future Works

This research proposes a first order discrete-time disturbance observer in the form of a Lie group variational integrator with finite-time convergence to the unknown dynamics. The observer design is shown to be nonlinearly stable and robust in estimating the disturbances in real-time. The observer design makes the observer estimation error to converge to a bounded neighborhood of zero. A comprehensive simulation study for the observer design is carried out for performance validation. In future works, asymptotically stable or finite-time robustly stable control schemes can be made to run in conjunction to formulate a unified data-driven robust feedback control scheme. Also, the LGVI discretization schemes will be derived for the case of variable time steps. Another important part of the analysis which will be carried in a later work is the examination of the bounds on the estimation errors for the disturbance force and torque in the presence of measurement noise in the true outputs. Finite-time stability and transient performance of the proposed observer can also be compared with similar fixed-time stable schemes, to compare their performance.

REFERENCES

[1] A. Soderlund, M. Kumar, and C. Yang, *Autonomous Wildfire Monitoring Using Airborne and Temperature Sensors in an Evidential Reasoning Framework*. [Online]. Available: https://arc.aiaa.org/doi/abs/10.2514/6.2019-2263

[2] A. A. Soderlund, M. Kumar, and R. Aggarwal, *Estimating the Real-time Spread of Wildfires with Vision-Equipped UAVs and Temperature Sensors via Evidential Reasoning*. [Online]. Available: https://arc.aiaa.org/doi/abs/10.2514/6.2020-1197

[3] L. H. Keel and S. P. Bhattacharya, "Controller synthesis free of analytical models: Three term controllers," vol. 53, pp. 1353–1369, 2017.

[4] N. J. Killingsworth and M. Krstic, "Pid tuning using extremum seeking: online, model-free performance optimization," vol. 26, pp. 70–79, 2006.

[5] L. dos Santos Coelho, M. P. Wicthoff, R. R. Sumar, and A. A. R. Coelho, "Model-free adaptive control design using evolutionary-neural compensator," *Expert Systems with Applications*, vol. 37, pp. 499–508, 2010.

[6] S. Syafiie, F. Tadeo, E. Martinez, and T. Alvarez, "Model-free control based on reinforcement learning for a wastewater treatment problem," *Applied Soft Computing*, vol. 11, pp. 73–82, 2011.

[7] Q. Ren and P. Bigras, "A highly accurate model-free motion control system with a Mamdani fuzzy feedback controller combined with a TSK fuzzy feed-forward controller," vol. 86, no. 3, pp. 367–379, 2017.

[8] J. Coulson, J. Lygeros, and F. Dörfler, "Data-enabled predictive control: In the shallows of the deepc," in *2019 18th European Control Conference (ECC)*. IEEE, 2019, pp. 307–312.

[9] T. Polóni, U. Kalabić, K. McDonough, and I. Kolmanovsky, "Disturbance canceling control based on simple input observers with constraint enforcement for aerospace applications," in *2014 IEEE Conference on Control Applications (CCA)*, 2014, pp. 158–165.

[10] T. Polóni, I. Kolmanovsky, and B. Rohaľ-Ilkiv, "Simple Input Disturbance Observer-Based Control: Case Studies," *Journal of Dynamic Systems, Measurement, and Control*, vol. 140, no. 1, 09 2017, 014501. [Online]. Available: https://doi.org/10.1115/1.4037298

[11] W.-H. Chen, J. Yang, L. Guo, and S. Li, "Disturbance-observer-based control and related methods—an overview," *IEEE Transactions on Industrial Electronics*, vol. 63, no. 2, pp. 1083–1095, 2016.

[12] D. Lee, "Nonlinear disturbance observer-based robust control of attitude tracking of rigid spacecraft," *Nonlinear Dynamics*, vol. 88, pp. 1317–1328, 2017.

[13] C. D. Johnson, "Real-time disturbance-observers; origin and evolution of the idea part 1: The early years," in *2008 40th Southeastern Symposium on System Theory (SSST)*, 2008, pp. 88–91.

[14] M. Chen, S. Xiong, and Q. Wu, "Tracking flight control of quadrotor based on disturbance observer," *IEEE Transactions on Systems, Man, and Cybernetics: Systems*, vol. 51, no. 3, pp. 1414–1423, 2021.

[15] S. P. Bhat and D. Bernstein, "Finite-time stability of continuous autonomous systems," *SIAM Journal on Control and Optimization*, vol. 38, no. 3, pp. 751–766, 2000.

[16] A. K. Sanyal and J. Bohn, "Finite-time stabilisation of simple mechanical systems using continuous feedback," *Int. J. Control*, vol. 88, no. 4, pp. 783–791, 2015.

[17] A. K. Sanyal, "Discrete-time data-driven control with hölder-continuous real-time learning," *International Journal of Control*, pp. 1–13, 2021. [Online]. Available: https://doi.org/10.1080/00207179.2021.1901993

[18] M. Fliess and C. Join, "Model-free control," vol. 86, no. 12, pp. 2228–2252, 2013.

[19] T. Lee, M. Leok, and N. Mcclamroch, "Lie group variational integrators for the full body problem in orbital mechanics," *Celestial Mechanics and Dynamical Astronomy*, vol. 98, pp. 121–144, 06 2007.

[20] R. Hamrah, A. K. Sanyal, and S. P. Viswanathan, "Discrete finite-time stable attitude tracking control of unmanned vehicles on SO(3)," in *2020 American Control Conference (ACC)*, 2020, pp. 824–829.

[21] N. Nordkvist and A. K. Sanyal, "A Lie group variational integrator for rigid body motion in SE(3) with applications to underwater vehicle dynamics," in *49th IEEE Conference on Decision and Control (CDC)*, 2010, pp. 5414–5419.

[22] A. Bloch, J. Baillieul, P. Crouch, and J. Marsden, *Nonholonomic Mechanics and Control, ser. Interdisciplinary Applied Mathematics*. Springer, Verlag, 2003.

[23] N. A. Chaturvedi, A. K. Sanyal, and N. H. McClamroch, "Rigid-body attitude control," *IEEE Control Systems Magazine*, vol. 31, no. 3, pp. 30–51, 2011.

[24] A. K. Sanyal and N. Nordkvist, "Attitude state estimation with multi-rate measurements for almost global attitude feedback tracking," vol. 35, no. 3, pp. 868–880, 2012.

[25] S. Bonnabel, P. Martin, and P. Rouchon, "Non-linear symmetry-preserving observers on Lie groups," *IEEE Transactions on Automatic Control*, vol. 54, no. 7, pp. 1709–1713, 2009.

[26] A. Khosravian, J. Trumpf, R. Mahony, and C. Lageman, "Observers for invariant systems on lie groups with biased input measurements and homogeneous outputs," *Automatica*, vol. 55, 05 2015.

[27] R. Mahony, T. Hamel, and J.-M. Pflimlin, "Nonlinear complementary filters on the special orthogonal group," *IEEE Transactions on Automatic Control*, vol. 53, no. 5, pp. 1203–1218, 2008.

[28] J. F. Vasconcelos, R. Cunha, C. Silvestre, and P. J. R. Oliveira, "A nonlinear position and attitude observer on SE(3) using landmark measurements," *Syst. Control. Lett.*, vol. 59, pp. 155–166, 2010.

[29] A. K. Sanyal, T. Lee, M. Leok, and N. H. McClamroch, "Global optimal attitude estimation using uncertainty ellipsoids," *Systems Control Letters*, vol. 57, no. 3, pp. 236–245, 2008. [Online]. Available: https://www.sciencedirect.com/science/article/pii/S016769110700120X

[30] S. Berkane and A. Tayebi, "On the design of attitude complementary filters on SO(3)," *IEEE Transactions on Automatic Control*, vol. 63, no. 3, pp. 880–887, 2018.

[31] M.-D. Hua, T. Hamel, R. Mahony, and J. Trumpf, "Gradient-like observer design on the special euclidean group SE(3) with system outputs on the real projective space," in *2015 54th IEEE Conference on Decision and Control (CDC)*, 2015, pp. 2139–2145.

[32] M.-D. Hua, G. Ducard, T. Hamel, and R. Mahony, "Introduction to nonlinear attitude estimation for aerial robotic systems," *Onera AerospaceLab Journal*, vol. Volume 8, 12 2014.

[33] V. S. Varadarajan, *Lie Groups, Lie Algebras, and Their Representations*. Springer New York, 1984. [Online]. Available: https://doi.org/10.1007%2F978-1-4612-1126-6

[34] R. M. Murray, *A Mathematical Introduction to Robotic Manipulation*. CRC Press, 1994.

[35] M. Izadi and A. K. Sanyal, "Rigid body pose estimation based on the lagrange-d'alembert principle," *Automatica*, vol. 71, pp. 78–88, 2016.

[36] S. Krishnaswamy and M. Kumar, "Tensor decomposition approach to data association for multitarget tracking," *Journal of Guidance, Control, and Dynamics*, vol. 42, no. 9, pp. 2007–2025, 2019. [Online]. Available: https://doi.org/10.2514/1.G004122